Generation of Simulated Earthquake Ground Motions Considering Target Response Spectra of Various Damping Ratios

J. Kanda, R. Iwasaki
Dept. of Building Engineering, University of Tokyo, 7-3-1 Hongo, Bunkyo-ku, Tokyo 113, Japan

Y. Ohsaki
Shimizu Construction Co., Ltd., 16-1 Kyobashi, 2-chome, Chuo-ku, Tokyo 104, Japan

T. Masao
Nuclear Power Plant Civil and Architecture Dept., Fujita Corporation, 74 Oodona, Kohoku-ku, Yokohama 223, Japan

Y. Kitada
Nuclear Engineering Dept., Nippon Atomic Industry Group Co., Ltd., 4-1 Ukishima-chyo, Kawasaki-ku, Kawasaki 210, Japan

K. Sakata
Nuclear Engineering Section, Toshiba Corporation, 8 Shinsugita, Isogo-ku, Yokohama 235, Japan

SUMMARY

It has been pointed out that the phase content in earthquake ground motions has a significant role in determining their non-stationary characteristics. As a typical example, the probability distribution of phase differences represents the envelope form of recorded motion. An alternative method, called the phase difference method, has been proposed for generating a spectrum-consistent simulated earthquake motion.

In this method, the Fourier phase angle components are generated to satisfy a specified probability distribution of phase differences and the convergence in the iterative computation process to fit the response spectrum of simulated earthquake motion to a target spectrum of a specified damping ratio, say 5%, is improved. However, when the response spectra for lower damping ratios are compared, the simulated spectra tend to be greater than the target spectra. This paper provides a methodology for generating simulated earthquake grond motions, whose response spectra of different damping ratios are fitted to respective target response spectra.

A parametric study was performed to investigate the influence of phase difference probability distribution breadth upon the low damping response spectra. Then, it was found that the greater the phase difference distribution breadth, the higher the 1% response spectrum value tends to be, while the simulated motion 5% response spectrum is well matched to that for the target.

In practical procedures, narrower phase difference distributions in several frequency bands can be employed to reduce the response spectrum value for low damping without changing the time history envelope form. This technique could lead to considerable improvement in fitness to the target response spectra with various damping ratios, which was confirmed in comparison with a simulated motion generated by the conventional method and one generated by utilizing the impulse phase for a certain frequency range. These simulated motions are exemplified in figures showing time histories and response spectra and also in terms of floor response spectra for a nuclear power plant.

1. Introduction

In the earthquake resistant design procedure for structures which require a higher safety standard and ability to withstand intense earthquake motions, such as is true for nuclear power plant buildings, the selection of appropriate earthquake motion data to be input into the design criteria is one of the most important problems for structural designers. In recent years, spectrum-consistent simulated eartuquake ground motions have been proposed considering the hypocentral distance and the earthquake magnitude corresponding to the construction site for a structure. These simulated motions are regarded as more rational structural design input data than existing natural earthquake motion records.

However, these simulated motions, generated to meet a target response spectrum with a specified damping ratio (e.g. 5%), tend to produce greater values for response spectra with lower damping than those for the target response. In other words, these simulated earthquake motions could cause an extraordinarily high response for vibrational systems with short natural periods and low damping ratios, such as equipments and piping systems in nuclear power plants.

When a simulated earthquake ground motion is generated, the non-stationary characteristics in the natural earthquake motions should be taken into account and should be represented in the simulated motion. Since the phase content in earthquake ground motions has a significant role in determining their non-stationary characteristics, the proper representation of the phase content should be a necessary condition for the proper generation of a simulated earthquake ground motion. As a typical example for the role played by the phase content, it has been found [1] that the probability distribution for phase differences determines the wave-shape or envelope function of motion.

This paper proposes a methodology for the generation of simulated earthquake ground motions whose response spectra of various damping ratios are matched to the target spectra of respective damping ratios by utilizing the phase difference distribution concept.

2. Conventional Method for Generating Simulated Earthquake Ground Motions.

A simulated earthquake motion can be generated by a superimposition of sinusoidal waves multiplied by a specified envelope function with random Fourier phase angles, whose Fourier amplitudes are iteratively determined to meet a specified target response spectrum. This methods is called the Sinusoidal Wave Superimposition Method (SWSM). The standard target response spectrum used in this work is the Ohsaki spectrum [2] with earthquake magnitude M=7, epicentral distance Δ = 20km, focal depth D = 5km and damping ratio h=5%. The target spectrum with a different damping ratio can be defined by an empirical form [3] as,

$$S_v^T(h) = R(n,h)\ S_v^T(5\%) \tag{1}$$

where

$$R(n,h) = \begin{cases} 1/\sqrt{1+17(h-0.05)\exp(-2.5/nT_D)} & \text{for } \frac{1}{n} > 0.07 \text{ sec.} \\ 1.0 & \text{for } \frac{1}{n} = 0.02 \text{ sec.} \end{cases}$$

$S_v^T(h)$ is the target response spectrum for damping ratio h.

n is the frequency (Hz) and T_D is the duration time in seconds.

An example wave, generated by the SWSM to meet $S_v^T(1\%)$, is shown in Fig. 1 together with its response spectrum for 5% damping, $S_V(5\%)$, and 1% damping, $S_V(1\%)$, and corresponding

target spectra $S_V^T(5\%)$ and $S_V^T(1\%)$, respectively. The envelope function used in this example is shown in Fig. 2. Duration time is 20.48 seconds, sampling time is 0.02 seconds and there are 1024 sinusoidal (Fourier) components. As observed in Fig. 1(b), $S_V(1\%)$ is rather greater than $S_V^T(1\%)$, in spite of the satisfactory $S_V(5\%)$ matching to target $S_V^T(5\%)$ shown in Fig.1(a).

In order to clarify this tendency, three quantities are defined as follows,

$$\mathrm{Err} = \sqrt{\overline{\left(\frac{S_V(h) - S_V^T(h)}{S_V^T(h)}\right)^2}} \tag{2}$$

$$\mathrm{Ave} = \overline{\left(\frac{S_V(h)}{S_V^T(h)}\right)} \tag{3}$$

$$\mathrm{Emax} = \left(\frac{\left|S_V(h) - S_V^T(h)\right|}{S_V^T(h)}\right)_{max} \tag{4}$$

Err , which represents the total matching factor or r.m.s. error, is 0.366 for h=1% (0.034 for h=5%), Ave , which represents the average relative to the target, is 1.286 for h=1% (1.006 for h=5%), and the maximum relative error, Emax , is 1.892 for h=1% (0.254 for h=5%). This is a typical example, which demonstrates that a simulated earthquake ground motion, generated to meet $S_V^T(5\%)$, produces a greater response spectrum with a lower damping ratio S_V (1%) than a target S_V^T (1%) estimated from eq.(1).

3. Relationship between Phase-Difference Distribution and Variation in Response Spectra with Damping Ratio

The SWSM does not require any explicit conditions for Fourier phase angles, only the envelope function determines its non-stationarity. It is revealed, however, that the envelope wave form can be obtained from the phase difference distribution, which is defined as the probability distribution for the differences between adjoining Fourier phase angle components. Namely, the phase difference distribution defines the superimposing method for consecutive Fourier components and then determines the wave form. Instead of multiplying the envelope function in the SWSM, the phase difference distribution, corresponding to the specified envelope function, can be introduced to improve the convergence in the generation of simulated earthquake motions [2].

Then, the relationship between the breadth of the phase difference distribution and the variation in response spectra with changing damping ratio, was parametrically studied. The phase difference distribution shape was postulated to be rectangular with breadth in this study, as shown in Fig. 3, for simplification. Simulated earthquake motions were generated with a phase difference distribution of breadth B to have the 5% phase difference distribution response spectrum matching S_V^T (5%) of the Ohsaki spectrum. The results are shown in Fig. 4 for B varying from 0 to 2π (four typical cases are presented, i.e. $B = \frac{\pi}{8}, \frac{\pi}{4}, \frac{\pi}{2}, \pi$). B = 0 corresponds to the phase distribution for an impulse wave. The wave form envelope becomes wider when breadth B for the phase difference distribution increases and the 1% response spectrum becomes greater. The increment rate of $S_V(1\%)$ is not uniform for all

frequency ranges. In a high frequency range, $S_v(1\%)$ tends to be greater than $S_v^T(1\%)$ at around $B=\pi/2$. Then, when $B \geqq \pi$, $S_v(1\%)$ becomes greater than $S_v^T(1\%)$ in any frequency range.

In order to investigate this tendency in more detail, the relationship between B and Err for 1% damping and between B and Ave for 1% damping for three frequency ranges, i.e. 0.5 Hz to 2.0 Hz, 2.0 Hz to 10.0 Hz and 10.0 Hz to 25.0 Hz were plotted in Fig. 5. Fig. 5(a) shows that the minimum Err occurs approximately at $\frac{\pi}{8}$ and $\frac{\pi}{2}$ for the 10.0 Hz to 25.0 Hz and the 2.0 Hz to 10.0 Hz frequency ranges respectively. Err values for the 0.5 Hz to 2.0 Hz range vary only insignificantly between $B=\frac{\pi}{2}$ and 2π. Err for the whole frequency range shows a similar tendency to that of Err for a high frequency range.

Figure 5(b) shows that Ave increases with B and crosses unity for the 10.0 Hz to 25.0 Hz high frequency range first at around $B=\frac{\pi}{8}$, then for the 2.0 Hz to 10.0 Hz frequency range at around $B=\frac{\pi}{3}$ and finally for the lower frequency range. The Ave variation with B for the whole frequency range is also similar to that for a high frequency range. Err values for 5% damping and Ave for 5% damping are plotted in each figure for comparison. The $S_v(5\%)$ match to $S_v^T(5\%)$ is satisfactory as Err < 5% and Ave ≃ 1.01.

As a result of this parametric study, it was found that the 1% response spectrum for simulated earthquake ground motions could differ, even when their $S_v(5\%)$ is similarly well matched to $S_v^T(5\%)$. The $S_v(1\%)$ match to $S_v^T(1\%)$ depends on the breadth of phase difference distribution, B. The appropriate value for B, which provides the smallest Err value and the Ave value closest to unity, depends on the frequency range, when a rectangular phase difference distribution is assumed. The $S_v(1\%)$ variation with B, when $S_v(5\%)$ is matched to $S_v^T(5\%)$, is rather sensitive, especially for a higher frequency range, but is not very sensitive for a lower frequency range.

4. Improved Phase Differnce Method

In the phase difference method, a specified phase difference distribution is used to generate a set of phase differences as random variables to satisfy the distribution for the whole frequency range, then to determine a set of Fourier phase angles. From a comparison of the envelope function defined in Fig 2 and the rectangular phase difference distribution in Fig. 3, the simulated earthquake ground motion generated by the existing phase difference method, which is equivalent to the conventional SWSM, can be considered to have a rather large B value (say, on the order of π), and this large B value causes a higher $S_v(1\%)$ versus $S_v^T(1\%)$.

In order to reduce $S_v(1\%)$ without loosing the $S_v(5\%)$ match to $S_v^T(5\%)$ and without changing the envelope form, manipulating phase difference distribution breadth, B, was introduced to improve the phase difference method. Namely, narrow B values for high frequency ranges were employed to reduce $S_v(1\%)$ or minimize Err. Wide B values for low frequency ranges were chosen to keep the envelope form, as a wide B value does not make a significant $S_v(1\%)$ increase in a low freuquency range, as demonstrated in Fig. 5.

As an extreme case, $B=0$ for a 6 Hz to 14 Hz frequency range was employed to generate a simulated earthquake ground motion, whose response spectrum of 1% damping would be less than the target $S_v^T(1\%)$ defined by eq.(1) in the corresponding frequency range. The time history and response spectra of 5% damping and 1% damping are shown in Fig. 6. $S_v(1\%)$ values are considerably less between 6 Hz and 14 Hz than the target $S_v^T(1\%)$ but are rather greater in

other frequency ranges than the target, while the $S_v(5\%)$ is well matched to $S_v^T(5\%)$. This example may not be acceptable for practical application, since the phase contents in the frequency range between 6 Hz and 14 Hz can not be representative of a natural recorded motion.

An improved example for a simulated earthquake ground motin was generated by employing different narrow rectangular phase difference distributions for frequency bands greater than 3.0 Hz as listed in Table 1. Data are shown in Fig. 7, together with its response spectra. The mean positions, $\mu\Delta\phi$, for the phase difference distributions were specified so that the dominant portion of higher frequency components occur in front of that for lower frequency components. $S_v(1\%)$ in a low frequency range (say $f < 3$ Hz) is similar to that for the conventional method (Fig. 1), but is improved in high frequency ranges to be better matched to the target $S_v^T(1\%)$. The time history for this example is not much different from that for the conventional method, in terms of maximum acceleration and envelope form.

In order to clarify the $S_v(1\%)$ matching to $S_v^T(1\%)$, Err, Ave and Emax for 1% damping for three frequency ranges listed in Table 2 for three examples of simulated motions generated by (a) conventional SWSM, (b) method utilizing impulse phase angles for the frequency between 6 Hz and 14 Hz and (c) the present method with the phase difference distributions described in Table 1. Err values for the present method are small, except for a low frequency range. Ave values are close enough to unity. Especially in a high frequency range between 10 Hz and 25 Hz, Err of 1% damping is significantly improved from 43% of the conventional method to 16% of the present method, although, in some frequency bands, the response for 1% damping could be considered to be too small. This should be investigated further in detail in order to establish how to choose the frequency bands and the breadth value for phase difference distribution for each frequency band.

5. Simulated Earthquake Ground Motions Floor Response Spectra

As a practical application example, the floor response for simulated earthquake ground motions, generated by the methods mentioned above, were computed. A lumped mass model with a sway-rocking spring at the bottom was used to represent a BWR Mark I type nuclear power plant building, as shown in Fig. 8. Computed floor response spectra for 1% damping at nodal point 1, which corresponds to the upper surface of the base mat, are shown in Fig. 9. A considerable reduction in the floor response for a low damped system of a high natural frequency (say $f \simeq 10$ Hz to 20 Hz) can be expected when the simulated earthquake ground motion generated by the present method is applied, versus the case of that by the conventional SWSM. Then, seismic input force for the low damped system could be reduced by approximately 50%. The floor response by the simulated motion with impulse phase for the frequency between 6 Hz and 14 Hz is slightly peculiar, as the response is drastically reduced only in the corresponding frequency range.

6. Conclusion

An improved method to generate a simulated earthquake ground motion, whose response spectra can be matched to the target spectra for various damping ratios, is proposed utilizing the phase difference distribution concept.

A parametric study was performed to investigate the influence of phase difference

probability distribution breadth upon the response spectra for a lower damping ratio. Then, it was found that the greater the phase difference distribution breadth, the higher the 1% response spectrum value tends to be, while the 5% response spectrum for simulated motion is well matched to that for the target.

In practical procedures, narrower phase difference distributions in several frequency bands, especially in a higher frquency range, can be employed to reduce the response spectrum value for a low damping ratio without changing the envelope form in regard to time history. This technique leads to considerable improvement in matching the target response spectra with various damping ratios. This was confirmed in comparison of response spectra for different damping ratios as well as floor response spectra for a typical nuclear power plant building.

The authors acknowledge valuable suggestions and discussions by Mr. J. Kani, Mr. T. Matsumoto and Mr. K. Gunyasu, of Toshiba Corp., by Dr. T. Nomura of NAIG, and by Mr. K. Shioya and Mr.K. Naraoka of Shimizu construction Co. Ltd.

REFERENCES

/1/ Ohsaki, Y., "On the significance of phase content in earthquake ground motions", Earth. Eng. Str. Dyn. Vol. 7, pp. 427-439, (1979).
/2/ Hisada, T., Ohsaki, T., Watabe, M. and Ohta, T., "Design spectra for stiff structures on rock", Proc. 2nd Int. Conf. on Microzonation, Vol. III, San Francisco, Nov. 1978.
/3/ Ohsaki Y., Watabe, M. and Uchiki, T., "Relationship between damping factor and shape of response spectrum", Rep. Ann. Meeting Archit. Inst. Japan, Sept. 1978, pp. 607-608.

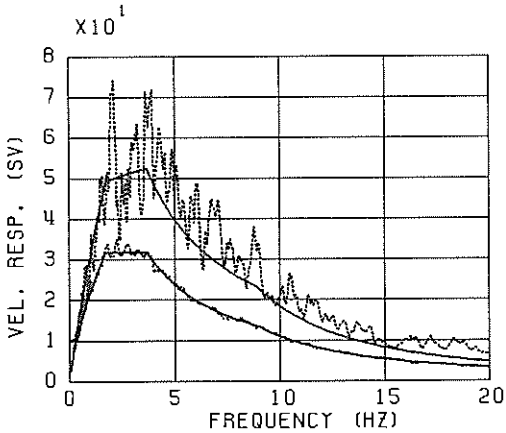

(a) response spectra

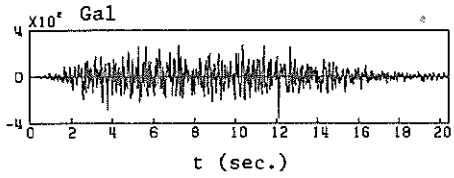

(b) time history

Fig.1 Simulated earthquake ground motion of M=7, Δ=20Km by SWSM.

$$e(t) = \begin{cases} (t/3.0)^2 & 0<t<3.0 \\ 1.0 & 3.0<t<12.5 \\ \exp[-0.1824(t-12.5)] & t>12.5 \end{cases}$$

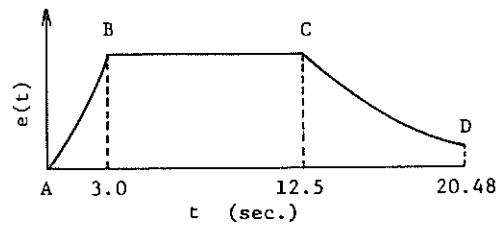

Fig.2 Envelope form used this study.

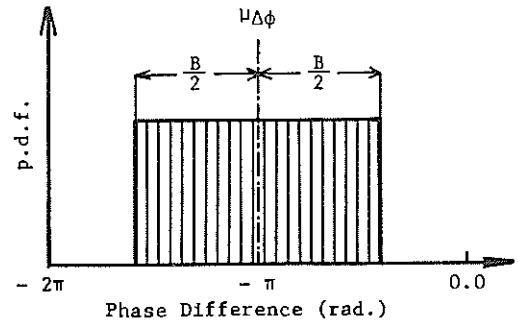

Fig.3 A rectangular distribution for the probability density of phase difference.

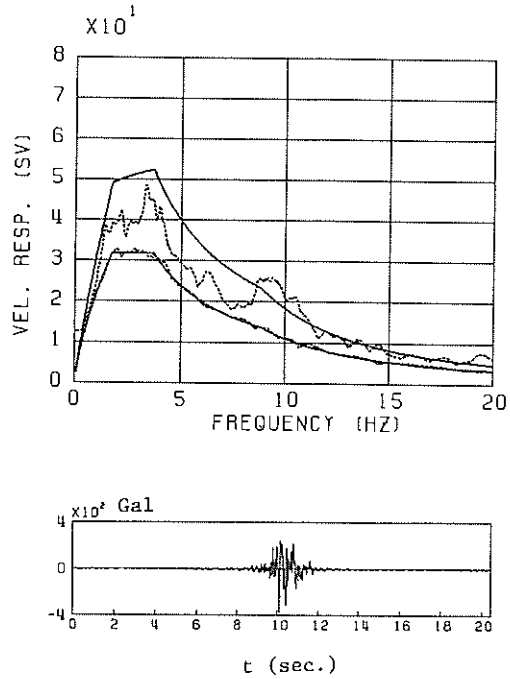

(a) $B = \frac{\pi}{8}$

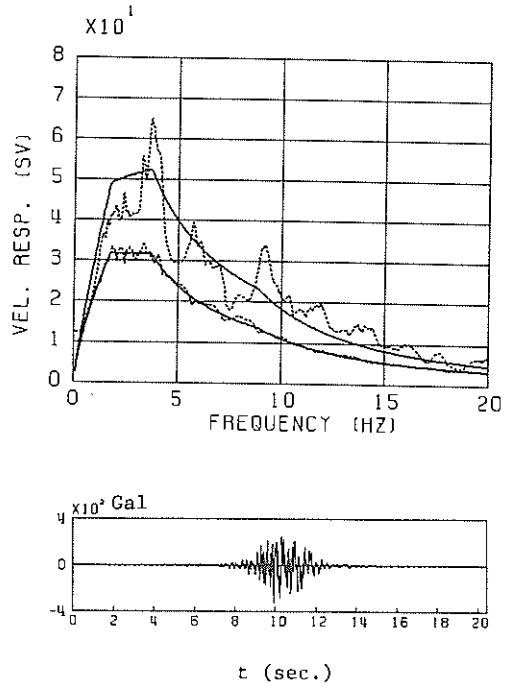

(b) $B = \frac{\pi}{4}$

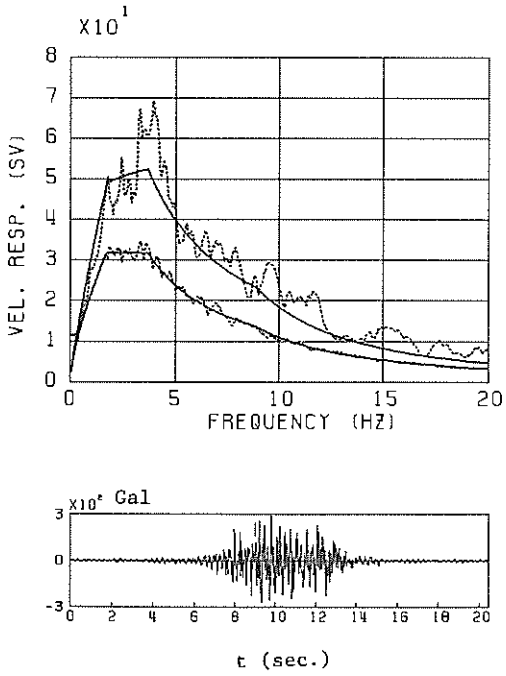

(c) $B = \frac{\pi}{2}$

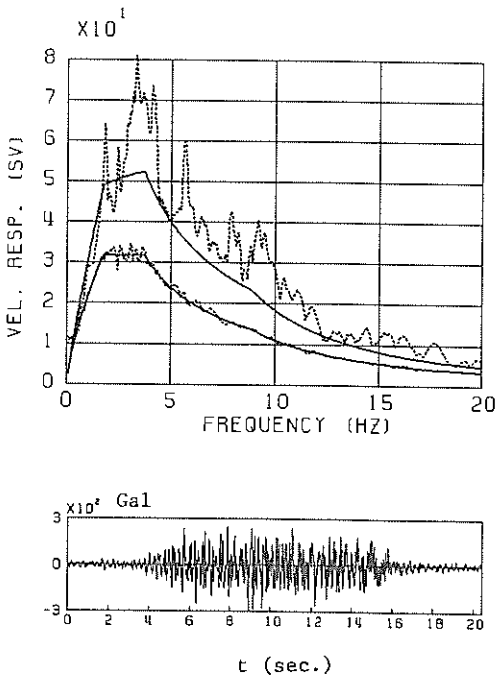

(d) $B = \pi$

Fig.4 Response spectra and time histories for simulated earthquake ground motions generated by the phase difference method with various B values.

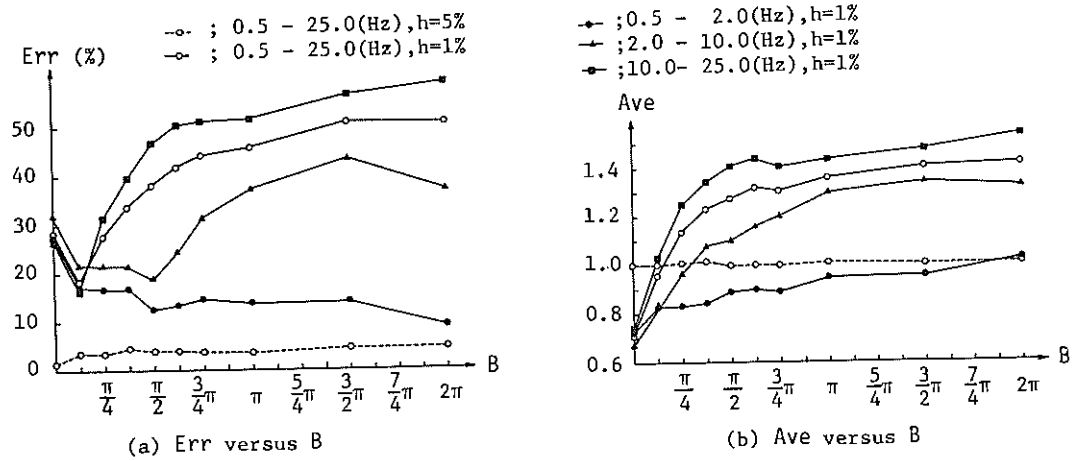

(a) Err versus B

(b) Ave versus B

Fig.5 Relationship between phase difference distribution breadth B and matching factors to the target response spectra.

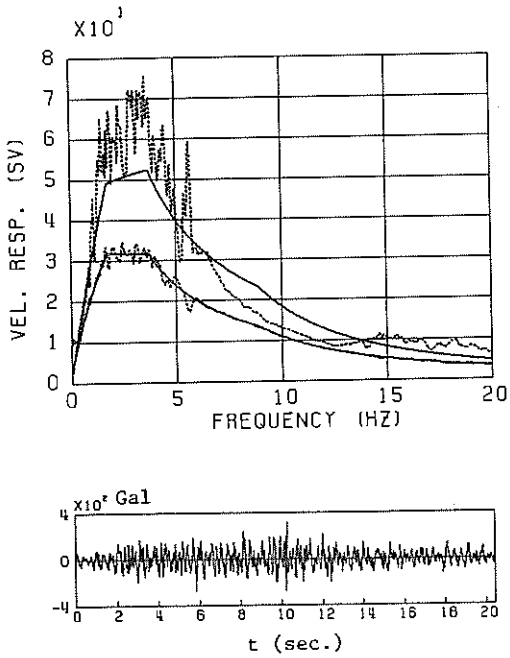

Fig.6 Simulated earthquake ground motion by employing the impulse phase in a frequency range between 6 Hz and 14 Hz.

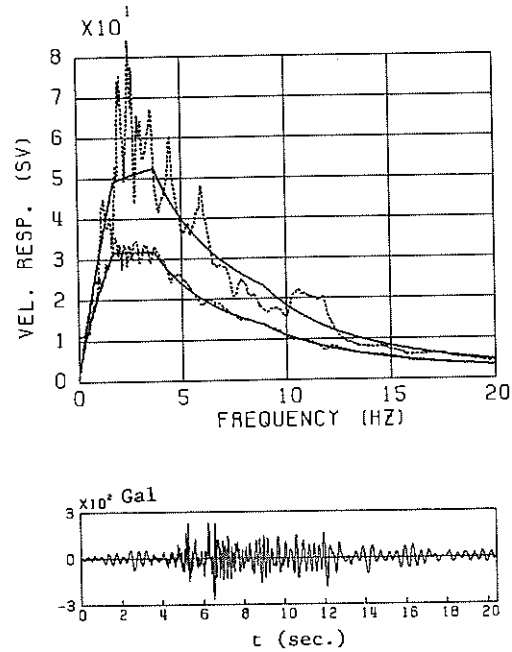

Fig.7 Simulated earthquake ground motion generated by the improved phase difference method.

Table 1. Parameters for Phase Difference Distribution Employed in The Improved Phase Difference Method

Frequency Band (Hz)	$\mu_{\Delta\phi}$ (rad.)	B (rad.)
3.0 - 4.4	-3.375	0.614
4.4 - 5.8	-2.761	0.614
5.8 - 11.7	-2.071	0.460
11.7 - 25.0	-1.611	0.153

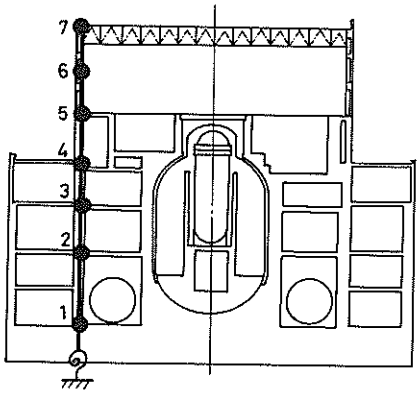

Fig.8 Lumped mass model for a BWR Mark I type nuclear power plant.

Table 2. Matching Factors of Simulated Earthquake Ground Motions by Various Methods to 1% Target Response Spectrum

(a) SWSM

Freq. Range (Hz)	Err	Ave	Emax
0.5 - 2.0	0.153	0.991	0.440
2.0 - 10.0	0.252	1.162	0.619
10.0 - 25.0	0.427	1.380	0.892
0.5 - 25.0	0.366	1.286	0.892

(b) Impulse Phase between 6 Hz and 14 Hz

Freq. Range (Hz)	Err	Ave	Emax
0.5 - 2.0	0.226	1.132	0.513
2.0 - 10.0	0.239	0.995	0.665
10.0 - 25.0	0.434	1.263	1.007
0.5 - 25.0	0.371	1.168	1.007

(c) Improved Phase Difference Method

Freq. Range (Hz)	Err	Ave	Emax
0.5 - 2.0	0.159	0.985	0.503
2.0 - 10.0	0.189	1.009	0.675
10.0 - 25.0	0.163	1.012	0.563
0.5 - 25.0	0.171	1.009	0.675

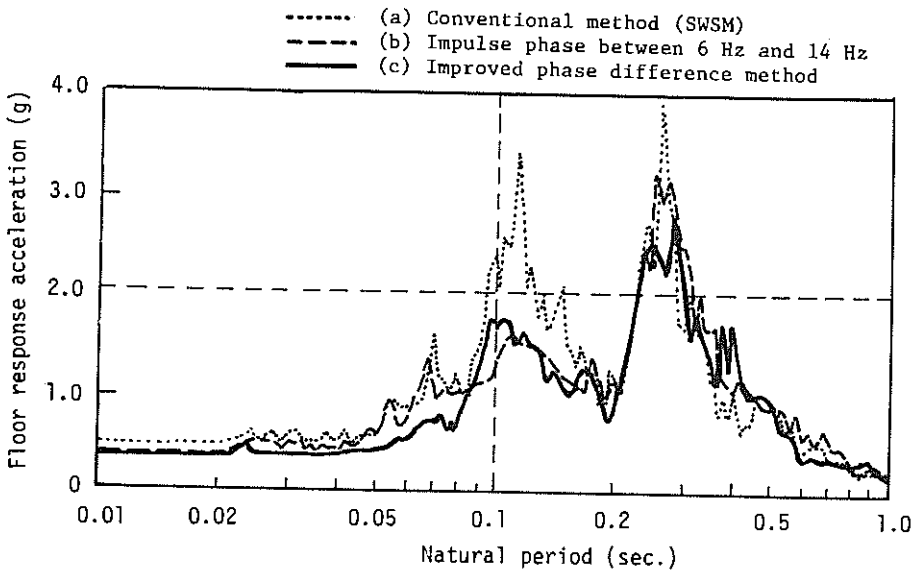

Fig.9 Floor response spectra of 1% damping at nodal point 1 for simulated earthquake ground motions generated by various methods.